Bioorganic & Medicinal Chemistry 21 (2013) 2733–2741

Contents lists available at SciVerse ScienceDirect

Bioorganic & Medicinal Chemistry

journal homepage: www.elsevier.com/locate/bmc

Metabolism of a potent neuroprotective hydrazide

Chandramouli Chiruta [a], Yanrong Zhao [b], Fangling Tang [b], Tao Wang [b], David Schubert [a,*]

[a] The Salk Institute for Biological Studies, La Jolla, CA 92037-1002, USA
[b] Pharmaron-Beijing, Beijing 100176, PR China

ARTICLE INFO

Article history:
Received 5 January 2013
Revised 23 February 2013
Accepted 3 March 2013
Available online 24 March 2013

Keywords:
Metabolites
Alzheimer's
Neuroprotective
Microsomes
Hydrazines

ABSTRACT

Using a drug discovery scheme for Alzheimer's disease (AD) that is based upon multiple pathologies of old age, we identified a potent compound with efficacy in rodent memory and AD animal models. Since this compound, **J147**, is a phenyl hydrazide, there was concern that it can be metabolized to aromatic amines/hydrazines that are potentially carcinogenic. To explore this possibility, we examined the metabolites of **J147** in human and mouse microsomes and mouse plasma. It is shown that **J147** is not metabolized to aromatic amines or hydrazines, that the scaffold is exceptionally stable, and that the oxidative metabolites are also neuroprotective. It is concluded that the major metabolites of **J147** may contribute to its biological activity in animals.

1. Introduction

There are currently no effective drugs that prevent the nerve cell death associated with Alzheimer's disease (AD), ischemic stroke, or any other age-associated neurodegenerative disease. To address this concern, we devised a drug discovery scheme based upon cell culture models of age-associated pathologies, such as the loss of nerve trophic factors, proteotoxicity, oxidative stress and reduced energy metabolism. A recent result of this program is a compound called **J147** (Fig. 3A). **J147** promotes memory in both normal rodents and AD mice, and limits synapse loss and pathology in AD animals.[1] **J147** is a hydrazide with the potential to be metabolized to aromatic amines or hydrazines,[2] a class of compounds with well-defined carcinogenic and toxic properties.[3–5] There are several FDA approved drugs that are aromatic hydrazones, such as the antihypertensive drug dihydralazine (for review, see[6]). However, because of the concern about the intrinsic stability of the hydrazone bridge and the production of aromatic amines/hydrazines from **J147**, its metabolites from both human and mouse microsomes were identified, synthesized, and assayed for biological activity in several neuroprotection assays. It is shown that the core structure of **J147** is stable in vivo, that no aromatic amines or hydrazines are produced, and that many of the metabolites have biological activities similar to **J147**.

2. Results and discussion

2.1. Microsomal metabolism of J147 in human and mouse liver microsomes

To determine the stability of **J147**, 5 μM **J147** was added to mouse or human whole blood and plasma, or microsomes plus or minus NADPH and the disappearance of **J147** monitored by LC–MS/MS. Figure 1 shows that **J147** is relatively unstable in human microsomes in the presence of NADPH. It has a half-life of 4.5 min in human microsomes and less than 4 min in mouse microsomes (not shown). To determine the metabolites, the reaction mixture was extracted after 5 min with ethyl acetate (**J147** is not very soluble in acetonitrile and strongly adheres to plastic) and run on a reverse-phase HPLC column. Figure 2 shows the HPLC profile before and after exposure to mouse (A and B) and human (C and D) microsomes.

The structures of the metabolites (**M1**, **M2**, **M3**, **M4** and **M5**) of **J147** were identified using a AB API4000 Q Trap LC/MS/MS instrument. To identify **J147** metabolites, the chromatographic and MS fragmentation behaviors of the parent compound were first investigated. The retention time of **J147** was 9.49 min (mouse) or 10.97 min (human) because different HPLC columns were used. In positive scan mode, **J147** formed a protonated molecule $[M+H]^+$ at *m/z* 351. Figure 3A shows the product ion spectrum of **J147** under the Enhanced Product Ion (EPI) scan. The fragments of **J147** were formed predominantly by the cleavage of the N–N and the C–F bond, resulting in product ions at *m/z* 136, 216, 200, 333 and 109. The CID pathways of **J147** were deduced and are

* Corresponding author. Tel.: +1 8584534100; fax: +1 8585359062.
E-mail address: schubert@salk.edu (D. Schubert).

0968-0896/$ - see front matter © 2013 Elsevier Ltd. All rights reserved.
http://dx.doi.org/10.1016/j.bmc.2013.03.020

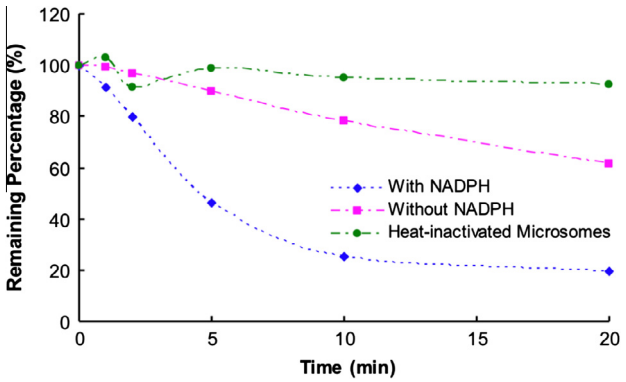

Figure 1. Metabolic stability of **J147** in human liver microsomes. Five micromolar **J147** was added to pooled human liver microsomes (0.5 mg/mL) in buffer plus or minus 1 mM NADPH, and the concentration of **J147** determined by LC/MS/MS. The percent remaining **J147** is plotted as a function of time.

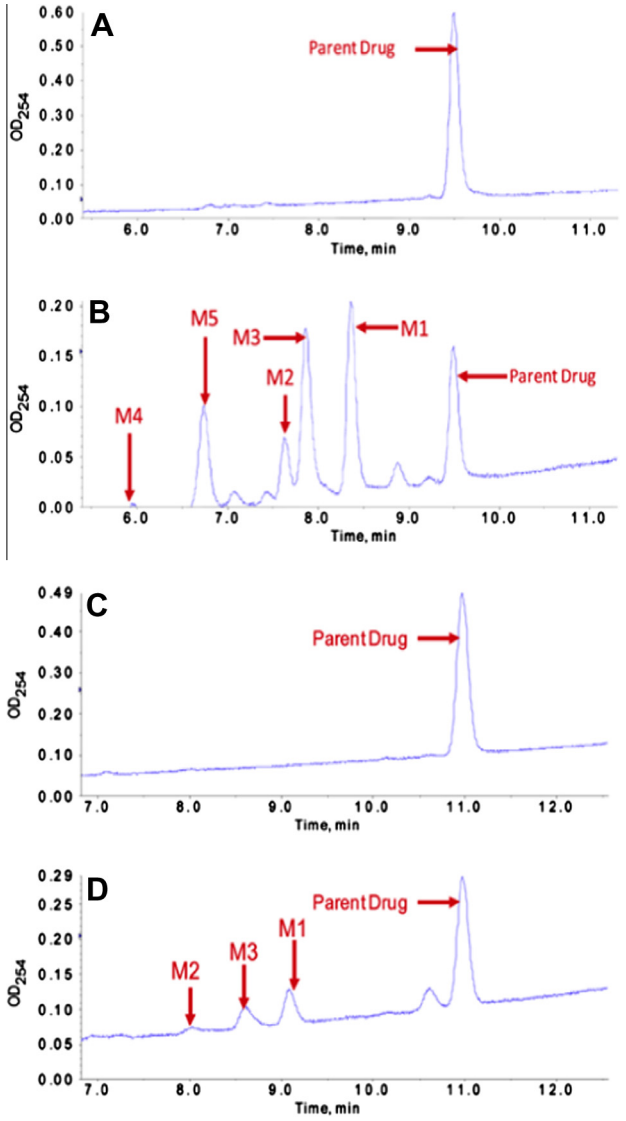

Figure 2. Separation of microsomal metabolic products: Five micromolar **J147** was incubated with mouse (A and B) or human (C and D) liver microsomes and extracted immediately at zero time (A and C) or after 5 min (B and D), followed by separation on a C18 reverse phase HPLC column. The fractions were collected, dried down, re-suspended in ethanol, and their biological activity determined in three neuroprotection assays (Fig. 7). Different HPLC columns were used for mouse and human material, therefore there are different elution times.

shown in Figure 3A. Using this fragment ion pattern, the mass spectra and chromatographic behaviors of the detected metabolites were compared with those of the parent compound and available authentic standards to characterize the metabolic structural modifications.

J147 metabolite (mouse) **M1**'s retention time is 8.36 min, exhibiting a protonated molecule m/z 337.1, with a mass shift of −14 Da relative to **J147** and metabolite (mouse) **M2**'s retention time is at 7.60 min, exhibiting a protonated molecule m/z 353, with a mass shift of 2 Da from **J147** and 16 Da from **M1**. Figure 3B and C shows the product ion spectrum of **M1** and **M2**, respectively under the EPI scan. The fragment ions of **M1** and **M2** at m/z 122, 138, 200, 216 and 218 were formed by the cleavage of the N–N bond. The fragment ions at m/z 319 and 335 were also observed by the cleavage of the C–F bond from **M1** and **M2**, respectively. The CID pathways of **M1** and **M2** were deduced and are shown in Figure 3B and C.

M3 (mouse) was identified as the oxidized metabolite of **J147** by addition of one hydroxyl group and exhibiting a protonated molecule m/z 367 with a retention time at 7.86 min. Metabolite **M4** (mouse) was identified as the demethylated and dioxidized metabolite of **J147** by removal of methyl and addition of two hydroxyls, and exhibiting a protonated molecule m/z 369 with a retention time at 5.96 min. **M5** (mouse) was identified as the dioxidized metabolite of **J147** by addition of two hydroxyls and exhibiting a protonated molecule m/z 383 with a retention time at 6.82 min. Fragment ions m/z 136, 216, m/z 138, 216, and m/z 152, 216 of **M3**, **M4** and **M5**, respectively were observed, which were the result of the N–N bond cleavage. The fragment ions m/z 337, 339 and 353, due to loss of CH_2OH and the fragment ions m/z 349, 351 and 365, due to loss of H_2O were observed for all three metabolites **M3**, **M4** and **M5**, respectively. A common fragment ion m/z 204 in all three metabolites **M3**–**M5** was observed by loss of CH_2OH followed by N–N bond cleavage from the corresponding parent molecules. The product ion spectra under EPI scan and CID pathways of **M3**, **M4** and **M5** are shown in Figure 4A–C.

The metabolites **M1**–**M5** of **J147** were also observed in the HPLC-UV chromatographs with similar retention times. In addition, these metabolites also showed similar isotope patterns in the Enhanced Resolution Scan (ER) compared with the parent compound (not shown).

A major goal of these studies was to determine if **J147** is metabolized to potentially toxic compounds such as 2,4-dimethylaniline (m/z = 121), 2,4-dimethylhydrazine (m/z = 136) or trifluoroacetamide hydrolysed product, 3-methoxy benzaldehyde (2,4-dimethylphenyl) hydrazone (m/z = 254). These compounds were not seen in either human or mouse microsomal preparations or mouse plasma following gavage of the drug.

Figure 5 summarizes the metabolites of **J147**. All are oxidation products of the aromatic rings; there was no indication that the hydrazone was cleaved, confirming that the molecular scaffold of **J147** is quite stable when incubated with microsomes. Only **M1** and **M3** were found in reproducible amounts in the metabolites of human microsomes (Fig. 2C and D), indicating a more limited metabolism by the human enzymes. The compound eluting just before **J147** in the human preparation (Fig. 2D) had the same mass as **J147** and was probably a stereoisomer of **J147**.

2.2. Blood metabolites of J147

Finally, because the metabolic products of **J147** from liver microsomes contain aromatic hydroxyl groups, it is possible that they become sulfated or glucuronidated in the blood. Therefore, the structural identification of the plasma metabolites in mice was examined. Figure 6 shows the blood and brain distribution of **J147** as a function of time following gavage of a 20 mg/kg in corn

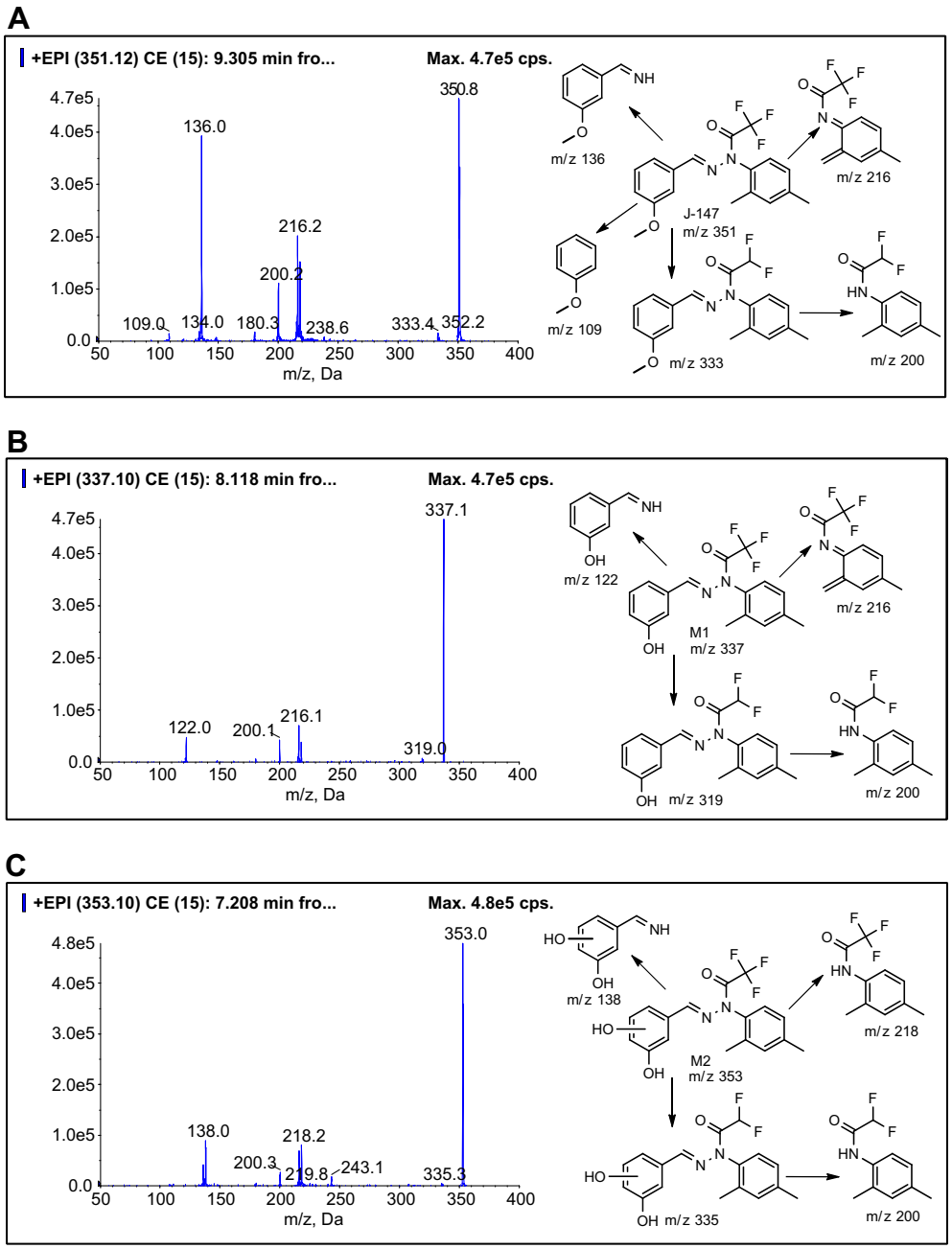

Figure 3. The product ion spectrums and proposed CID pathways of **J147** (A), **M1** (B), and **M2** (C) under the Enhanced Product Ion (EPI) scan.

oil. The peak concentration occurred around 2 h in both tissues with a half-life of 2.5 h. At all times, the tissue concentration was well above the EC_{50} of **J147** in our cell culture screening assays.[1] The structures of the metabolites were determined using the same methods as for the microsomal metabolites and are shown in Table 1. The two major metabolites had gains of sulfate and of glucuronic acid. A minor metabolite was a loss of a methyl group of **J147**.

2.3. Synthesis of J147, M1, M2 and M3

The synthesis of the metabolites was carried out in 2–3 steps using simple chemistry as described in our previous paper.[1] Hydrazones **1**, **2** and **5** were synthesized by condensation of appropriately substituted aldehydes and hydrazines in EtOH at room temperature (Scheme 1). Synthesis of intermediate hydrazides **3**, **6** and **J147** has been carried out by acetylation using trifluoroacetic anhydride and triethylamine in CH_2Cl_2 from the corresponding hydrazones. Finally, methyl and ethyl deprotection of **J147** and **3**, respectively was performed by iodocyclohexane in DMF to yield **M1** and **M2**. Metabolite **M3** was prepared from hydrazide **6** by reduction of methyl ester using DIBALH in dichloromethane. Hydrazine **4** prepared from the commercially available amine by $NaNO_2$ and $SnCl_2$ reaction (Scheme 1).

2.4. Neuroprotective activity of metabolites

To confirm the human microsomal metabolite structures by chemical synthesis and to provide sufficient material to further evaluate them in biological assays, human hepatic microsomal metabolites **M1**, **M2** and **M3** of **J147** were prepared and characterized by ^{1}H, ^{13}C NMR, LC/MS and ESI-MS analysis. There is a possibility of other *ortho*, *meta* hydroxylated isomers of **M2** and *ortho*

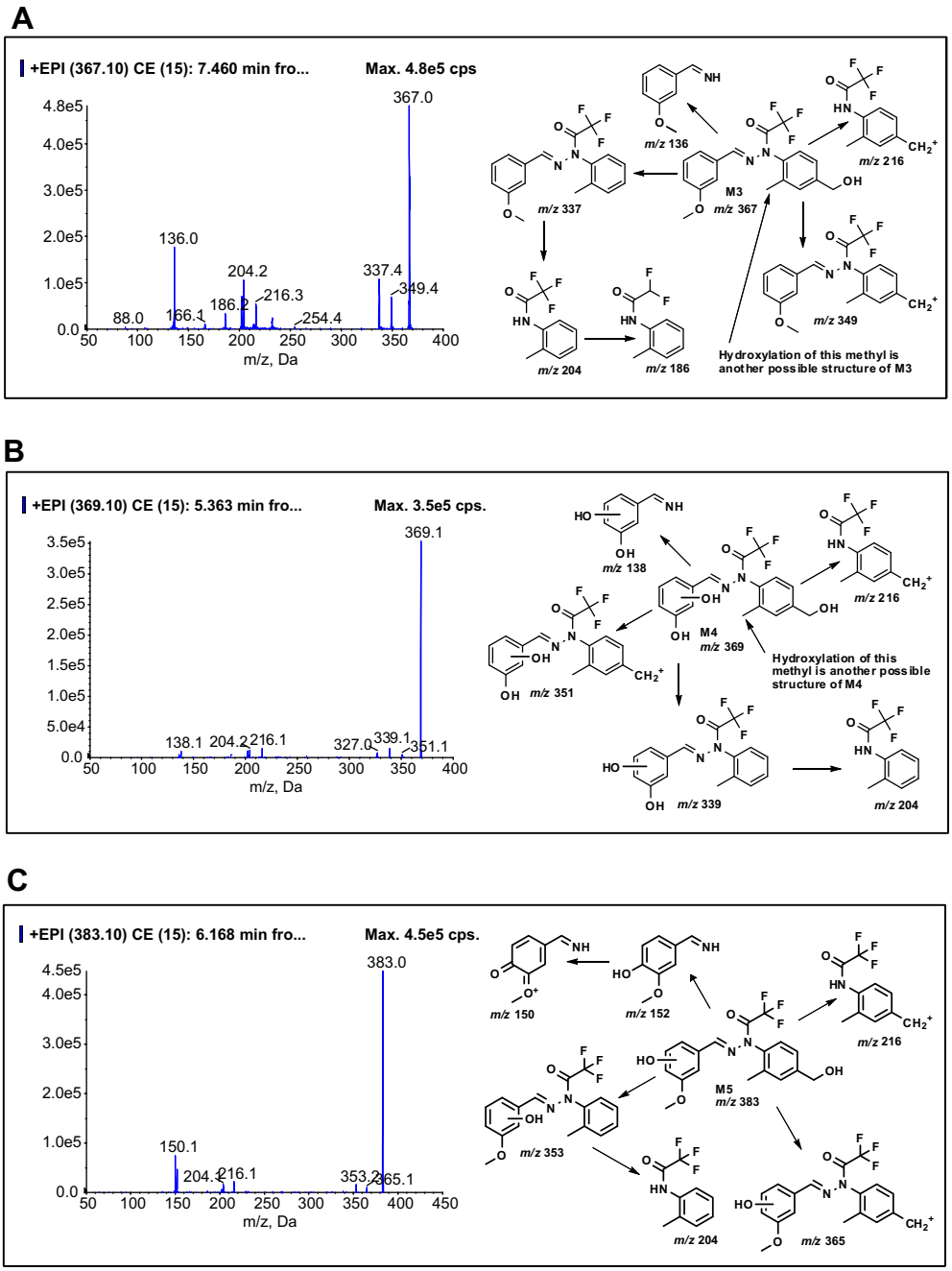

Figure 4. The product ion spectrums and proposed CID pathways of **M3** (A), **M4** (B) and **M5** (C) under the Enhanced Product Ion (EPI) scan.

hydroxymethyl isomer of **M3** (Figs. 3C and 4A). However, because the enzymatic hydroxylation is likely to take place at the para position due to steric and electronic factors around the aromatic ring, only the potential **M2** and **M3** metabolites with the para-hydroxy groups were made.[10,11] The exclusive formation of these **M2** and **M3** metabolites was confirmed by comparing them with the authentic samples isolated from microsomes by HPLC and TLC. All of the tested synthetic compounds have purity above 95%.

To determine if any of the breakdown products have biological activity, each of the three major peaks in the human microsome preparation were initially collected and measured for biological activity in three assays: (1) trophic factor withdrawal assay; (2) the ability to block intracellular Aβ toxicity; and (3) protection from oxidative stress. **M1**, **M2**, and **M3** isolated directly from microsomes were all active in these assays. Once their structures were determined and the compounds were synthesized, it was determined that most of the **J147** metabolites were biologically active in the neuroprotection assays (Fig. 7 and Table 2).

Trophic factors are greatly reduced in AD brain.[12] In our assay for trophic factor withdrawal (TFW), primary embryonic cortical cells are plated at low density in serum-free medium (Fig. 7A). At low density, the cells die within 2 days but can be rescued by combinations of neurotrophic growth factors, but not by one alone.[13] In contrast, cell death is prevented by **J147** alone with an EC_{50} of 33 nM. **M1** and **M2** were similarly active, but **M3** was 10-fold less active in this assay (Table 2).

Aβ is thought to be one of the toxic entities in AD, and the intracellular accumulation of Aβ and C-terminal amyloid precursor

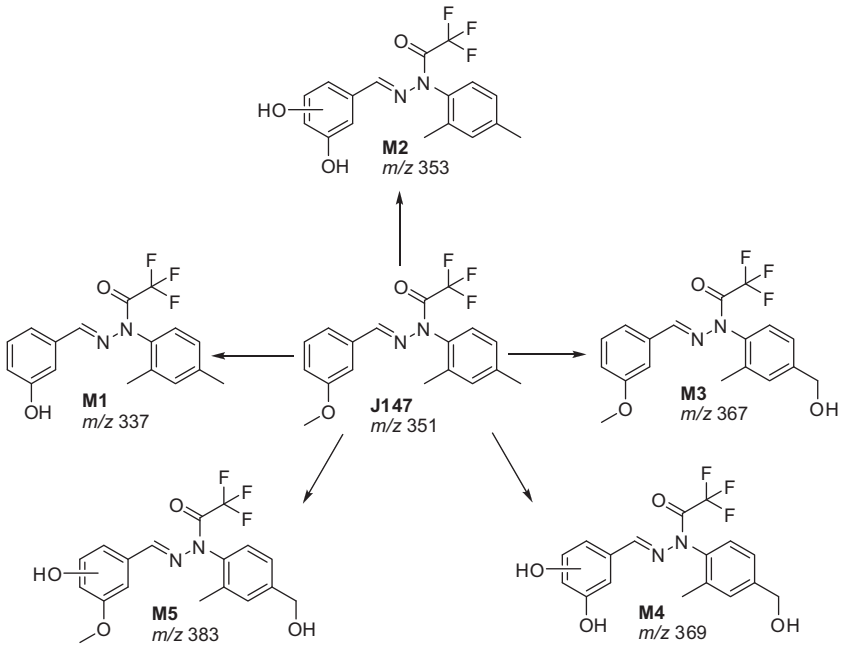

Figure 5. Metabolic products of **J147**.

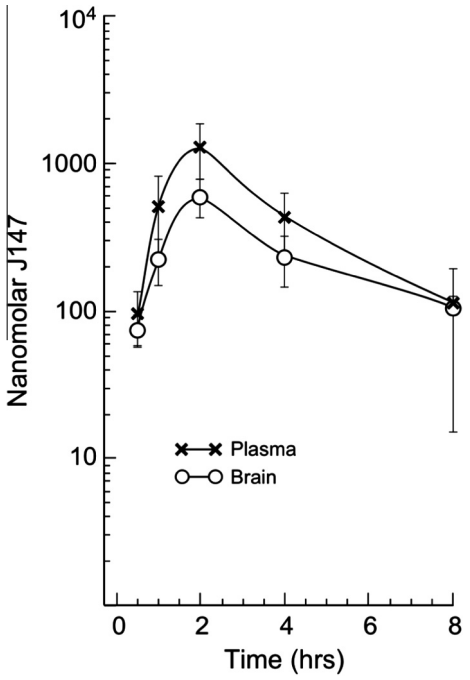

Figure 6. Pharmacokinetics of **J147** following a single gavage at 20 mg/kg in corn oil. Blood and brain distribution as a function of time. x–x, blood; o–o, brain. The data are presented as mean plus or minus the standard error of the mean. $N = 3$ per time point.

protein (APP) fragments are also toxic.[14,15] To determine if **J147** metabolites are able to inhibit intracellular Aβ toxicity, a human neuroblastoma cell line that conditionally expresses the C-terminal 99 amino acids (C99) derived from the β-secretase cleavage of APP was used. This cell line, called MC-65,[16] has recently been used to identify drugs that inhibit amyloid aggregation.[8] The cells are routinely grown in the presence of tetracycline and, following its removal, the expression of C99 is induced and the cells die within 4 days due to the accumulation of intracellular, toxic protein aggregates. Metabolites **M1**, **M2**, and **M3** all protect cells from intracellular Aβ toxicity with EC_{50}s below 100 nM (Fig. 7B and Table 2).

Many models of programmed cell death have been established to characterize the oxidative mechanisms underlying neuronal degeneration. One of the most robust of these models is the glutamate-induced programmed cell death of immature cortical neurons and of hippocampal HT22 nerve cells.[17,18] In this assay, elevated levels of extracellular glutamate interfere with cystine uptake through the cystine/glutamate antiporter, which normally carries cystine into cells at the expense of the outflow of glutamate. The decreased cystine uptake leads to the depletion of intracellular GSH, a cysteine-containing tripeptide vital for cell survival because of its ability to act as an enzymatic cofactor and antioxidant. This form of cell death, called oxytosis,[18] is distinct from excitotoxicity but is important to the understanding of neuronal degeneration in that it represents a form of oxidative stress common to all CNS diseases. Figure 7C and Table 2 show that **J147** metabolites are much less neuroprotective in this assay than **J147**, perhaps because they are more oxidized forms of **J147**.

3. Conclusions

The above data show that the microsomal metabolites of **J147** are oxidation products of the aromatic rings, that the hydrazone scaffold of the compound remains intact, and that the human microsomal metabolites are biologically active in the cell culture neuroprotection assays used to develop **J147** from its natural product parent molecule curcumin.[9,1] Although there is concern that hydrazones/hydrazides associated with aromatic rings can be metabolized to toxic amines/hydrazines,[10,11] none of the compounds were identified as either microsomal or blood metabolites. Hydrolysis of trifluoroacetamide was also not observed. While it is clearly impossible to say that none were produced, based upon the technology that was used, they must constitute less than 5% of the total. If there is no hydrolysis of the amide there will be no formation of hydrazone and no further breakdown into amine/hydrazine derivatives, then the microsomal metabolites of **J147** are likely to be simple oxidation products of the aromatic rings. This prediction

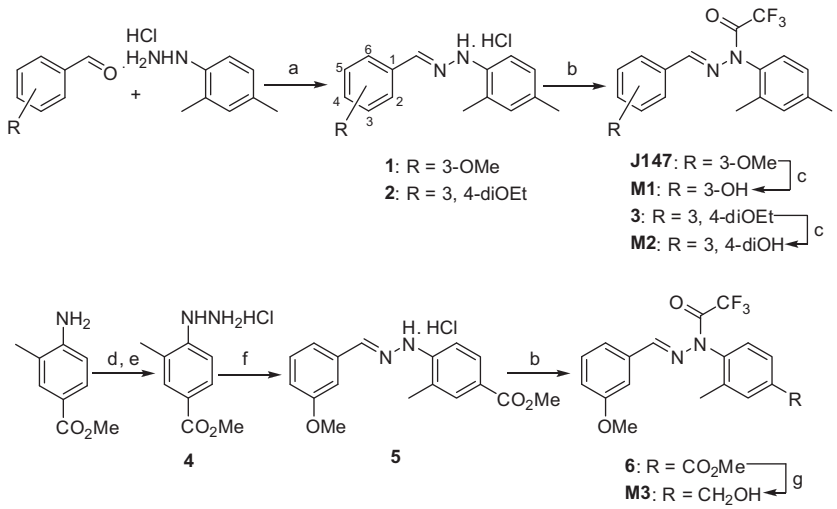

Scheme 1. Reagents and conditions: (a) EtOH, rt, 1–5 h, 80–90%; (b) Et_3N, $(CF_3CO)_2O$, CH_2Cl_2, 0 °C, 1–5 h, 60–80%; (c) iodocyclohexane, DMF, reflux, 12 h, 60–70%; (d) $NaNO_2$, 6 N HCl, <15 °C, 1.5 h; (e) $SnCl_2$, 0–10 °C, 2 h, 80%; (f) 3-methoxybenzaldehyde, EtOH, rt, 5 h, 80%; (g) DIBALH, −78 °C, 2 h, 68%.

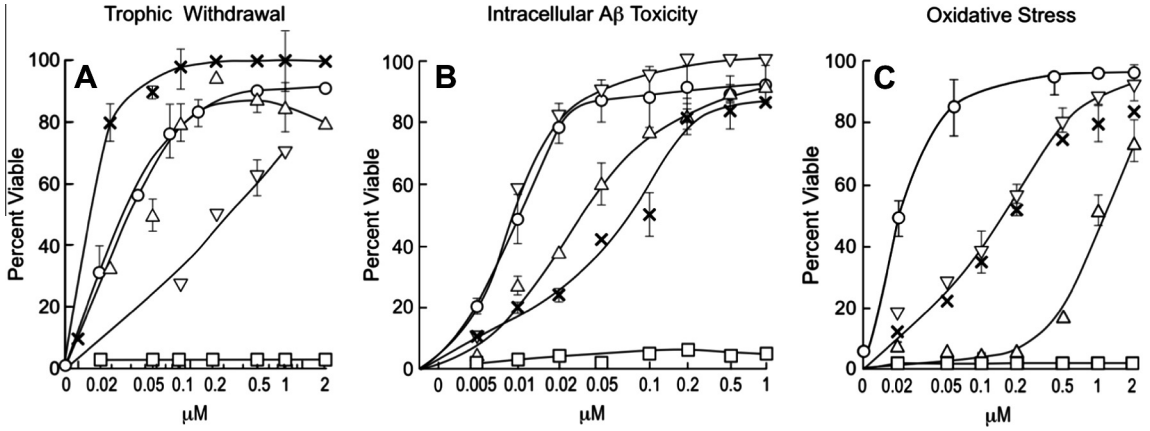

Figure 7. J147 metabolites are biologically active. Increasing concentrations of **J147** and its synthetic metabolites were assayed in three different assays for neuroprotection. In all cases, the assay outcome was protection from nerve cell death caused by the lack of trophic support (A), the toxicity of Aβ accumulation within cells (B), or oxidative stress caused by the loss of glutathione (C). The calculated EC_{50} values are shown in Table 2. × = **M1**; △ = **M2**; ▽ = **M3**; ○ = **J147**; □ = inactive analogue of **J147** in which both nitrogens are replaced by carbons.

Table 1
Mouse blood metabolites

Peak No.	Sample name	rt (min)	Expected (*m*/*z*)	Mass shift	Proposed biotransformation
1	**J147**	9.27	351.1	–	–
2	**BM1**	5.35	431.1	80	Sulfonation (Gain of 'SO_3')
3	**BM2**	5.54	513.2	162	Demethylation and glucuronidation (loss of 'CH_2' and gain of '$C_6H_8O_6$')
4	**M1**	8.04	337.1	−14	Demethylation (loss of 'CH_2')

Mice were given **J147** at 20 mg/kg iv and the **J147** metabolites in the blood assayed 20 min later by procedures described for microsomal metabolites. Phenomenex Synergi 4μ Polar-RP (50 × 2.00 mm) column used for analysis.

Table 2
Neuroprotective activities of **J147** and metabolites

Compound name	Trophic factor withdrawal	Intracellular Aβ toxicity	Oxidative stress
M1	0.012	0.078	0.185
M2	0.031	0.034	1.0
M3	0.320	0.092	0.180
J147	0.033	0.011	0.020

EC_{50} values (in μM) of neuroprotective activities of **J147** and metabolites.

was confirmed by the identification and synthesis of the human microsomal metabolites, as well as the observation of only sulfonated and glucuronidated products of the microsomes found in blood. The fact that the microsomal metabolites have similar biological activities as the parent drug and that they become sulfonated or glucoronidated in circulation argues that toxicity due to drug metabolism is unlikely to be an immediate concern with **J147**, but will require study during the Investigational New Drug Allowance and Phase 1 clinical trials.

4. Experimental section

4.1. Materials

Compounds **J147**, **M1**, **M2** and **M3** were synthesized in our laboratory at Salk Institute. All starting materials, chemicals, reagents were obtained from Sigma Aldrich, (Milwaukee WI), and used as received. Solvents used for synthesis and chromatographic analysis were HPLC or ACS reagent grade and were purchased from Fisher Scientific Co (Pittsburg, PA). Thin layer chromatography (TLC) used EMD silica gel F-254 plates (thickness of 0.25 mm). Flash chromatography used EMD silica gel 60, 230–400 mesh and were purchased from EMD Chemicals (San Diego, CA). MTT (3-(4,5 dimethylthiazol-2-yl)-2,5-diphenyltetrazolium bromide) for the bioassays was purchased from Sigma (St. Louis, MO). Liver microsomes from mouse and humans, DMEM/F12 medium N2 supplement and the live-dead assay kit (#L3224) were purchased from In Vitrogen (Carlsbad, CA).

4.2. Analytical methods

^{1}H NMR and ^{13}C NMR were recorded at 500 and 125 MHz, respectively, on a Varian VNMRS-500 spectrometer at the Salk institute (La Jolla, CA) using the indicated solvents. Chemical shift (δ) is given in parts per million (ppm) relative to tetramethylsilane (TMS) as an internal standard. Coupling constants (J) are expressed in hertz (Hz), and conventional abbreviations used for signal shape are as follows: s = singlet; d = doublet; t = triplet; m = multiplet; dd = doublet of doublets; br s = broad singlet. Liquid chromatography mass spectrometry (LCMS) was carried out using a Shimadzu LC-20AD spectrometer at The Scripps Research Institute (La Jolla, CA), and electrospray ionization (ESI) mass analysis with a Thermo Scientific LTQ Orbitrap-XL spectrometer at the Salk institute (La Jolla, CA). Melting points were determined with a Thomas-Hoover capillary melting point apparatus at the Salk institute (La Jolla, CA), and are uncorrected. All final compounds were characterized by LCMS and ^{1}H NMR and gave satisfactory results in agreement with the proposed structure. All of the tested compounds have a purity of at least 95% which was determined by analysis on a C18 reverse phase HPLC column [Phenomenex Luna (50 mm × 4.60 mm, 3 m)] at The Scripps Research Institute (La Jolla, CA), using 10–90% CH_3CN/H_2O containing a 0.02% AcOH with a flow rate of 1 mL/min (5 min gradient) and monitoring by a UV detector operating at 254 nm.

4.3. Metabolic determination

Mass spectra were acquired in the positive mode scanning over the mass range of 50–1000. LCMS M+H signals were consistent with the predicted molecular weights for the reported compounds. Metabolite analyses were performed on AB API4000 Q Trap LC/MS/MS spectrometer and HPLC Shimadzu (DGV-20A3), LC-20AD and CTC Analytics HTC PAL System at Pharmaron (Beijing, China). The HPLC column used was Phenomenex Synergi 4μ Polar-RP (50 × 2.00 mm) or a Phenomenex Luna 5 C18 (50 × 2.00 mm). HPLC resolution was achieved with a gradient consisting of solvent A (water–acetonitrile–formic acid, 95:5:0.1) and solvent B (water–acetonitrile–formic acid, 5:95:0.1) with 0.3 mL/min flow rate. The Luna column was used for the human microsomes (Fig. 2C and D) and the Polar-RP for mouse (Fig. 2A and B). Blood metabolites were analyzed on the Phenomenex Synergi 4μ Polar-RP (50 × 2.00 mm).

4.4. Microsomal stability

Microsomal stability assays were done in 5 mM phosphate buffer, pH 7.3, with or without 1 mM NADPH and 0.5 mg/mL human or mouse microsomes. In some cases heat-activated (98 °C, 10 min) microsomes were used as controls and verapamil was used as a control. At 0.1, 2, 5, 10 and 20 min at 37 °C the reaction was stopped with three volumes of ethyl acetate, centrifuged at 16,000 rpm for 15 min and an aliquot of the supernatant used for LC/MS/MS analysis. In some cases the individual metabolites were directly isolated from the HPLC run and assayed for biological activity.

4.5. Animal studies

Male Balb C mice were given a single dose by body weight intravenously at a volume of 5 mL/kg (1 mg/kg) or via oral gavage at a volume of 10 mL/kg (5 mg/kg). Blood samples were collected into Na-Heparin microtainer tubes for plasma separation. Blood samples were centrifuged at 4 °C at 6000 rpm for 5 min. Decanted plasma samples were stored at −80 °C until used. Brains were perfused and collected for the brain penetration. The tissue samples were stored at −80 °C. Plasma and brain samples were thawed on ice and kept at 4 °C during processing. Brain tissues were homogenized in PBS, pH 7.4. An aliquot of plasma or brain homogenate sample or calibration sample were mixed with three volumes of methanol containing internal standard, incubated on ice for 10 min, and centrifuged. The protein free supernatant was used for LC/MS/MS analysis.

4.6. Trophic factor withdrawal

Primary cortical neurons were prepared from 18-day-old rat embryos according to published procedures[7] and cultured at a low cell density of 1×10^6/35 mm dish in DMEM/F12 (2 mL) containing N2 supplement and the compounds to be assayed. Viability was assayed 2 days later using a fluorescent live-dead assay and the data presented as the percent of input cells surviving.

4.7. Intracellular amyloid toxicity

The induction of intracellular amyloid toxicity in MC65 cells was done exactly as described.[8] Briefly, cells from confluent cultures were dissociated and plated at 4×10^5 per 35 mm tissue culture dish in the presence (no induction) or absence (APP-C99 induced) of 1 g/mL tetracycline and in the presence or absence of the indicated compounds. At day 4 the control cells in the absence of tetracycline were dead, and cell viability was determined by the MTT assay.[9] The data are presented as viability relative to controls plus tetracycline.

4.8. Oxytosis assay

HT22 cells were plated at 2×10^3 cells per well in 96-well tissue culture dishes in DMEM plus 10% fetal calf serum. The following day the test compounds were added in triplicate at indicated concentrations. Thirty minutes after compound addition, 5 mM glutamate was added to initiate the cell death cascade. Twenty hour later, the MTT assay was performed. The results are presented as the percentage of survival relative to the controls with vehicle alone.

4.9. Synthesis of (*E*)-*N*-(2,4-dimethylphenyl)-2,2,2-trifluoro-*N*′-(3methoxybenzyli-dene) acetohydrazide (J147)

A mixture of 3-methoxybenzaldehyde (500 mg, 3.67 mmol) and (2,4-dimethylphenyl) hydrazine hydrochloride (632 mg, 3.67 mmol) in EtOH (10 mL) was stirred at room temperature for 1 h, obtained solid was filtered off, washed with ethanol and dried

under vacuum to afford hydrazone hydrochloride **1** (960 mg) in 90% yield as a light brown solid. This unstable hydrazone (570 mg, 1.96 mmol) was dissolved in CH_2Cl_2 (10 mL), Et_3N (0.54 mL, 3.93 mmol) followed by $(CF_3CO)_2O$ (0.27 mL, 1.96 mmol), was added at 0 °C and the mixture was stirred at room temperature for 1 h. Reaction mixture was diluted with aq satd $NaHCO_3$ solution (20 mL), extracted with CH_2Cl_2 (2 × 30 mL), dried (Na_2SO_4) and evaporated, resulting solid was recrystalized from ethanol to give **J147** (550 mg, 80%) as a white solid: mp 70–72 °C; LCMS purity 98%; ^{1}H NMR ($CDCl_3$, 500 MHz) δ ppm 2.09 (s, 3H), 2.42 (s, 3H), 3.83 (s, 3H), 6.95 (dd, J = 8.5, 2.0 Hz, 1H), 7.05 (d, J = 8.0 Hz, 1H), 7.13 (d, J = 7.5 Hz, 1H), 7.21 (d, J = 8.5 Hz, 1H) 7.24–7.30 (m, 4H); ^{13}C NMR ($CDCl_3$, 125 MHz) δ ppm 17.20, 21.50, 55.47, 111.97, 116.03, 117.40, 118.32, 121.23, 128.78, 128.97, 129.90, 129.99, 132.81, 134.95, 136.49, 141.16, 144.10, 160.22; MS (ESI): m/z calcd for $C_{18}H_{17}F_3N_2O_2$ ([M+H]$^+$) 351.1314; found 351.1366 ([M+H]$^+$).

4.10. Synthesis of (*E*)-*N*-(2,4-dimethylphenyl)-2,2,2-trifluoro-*N*′-(3-hydroxybenzyli-dene) acetohydrazide (M1)

J147 (410 mg, 1.17 mmol) and iodocyclohexane (0.30 mL, 2.34 mmol) in DMF (2 mL) was refluxed for 12 h. Reaction mixture was cooled and diluted with water, (10 mL), extracted with EtOAc (2 × 20 mL), washed with brine (20 mL), dried (Na_2SO_4) and evaporated, resulting solid was recrystalized from ethanol to give **M1** (250 mg, 63%) as a white solid: mp 151–153 °C; LCMS purity 99%; ^{1}H NMR ($CDCl_3$, 500 MHz) δ ppm 2.08 (s, 3H), 2.41 (s, 3H), 5.14 (s, 1H) 6.86 (dd, J = 7.5, 2.0 Hz, 1H), 7.03 (d, J = 8.0, Hz, 1H), 7.07 (d, J = 8.0 Hz, 1H), 7.21 (m, 5H); ^{13}C NMR ($CDCl_3$, 125 MHz) δ ppm 16.98, 21.31, 113.42, 118.04, 121.27, 128.50, 128.78, 130.04, 132.69, 134.81, 136.20, 141.01, 143.82, 156.02; MS (ESI): m/z calcd for $C_{17}H_{15}F_3N_2O_2$ ([M+H]$^+$) 337.1158; found 337.1203 ([M+H]$^+$).

4.11. Synthesis of (*E*)-*N*′-(3,4-dihydroxybenzylidene)-*N*-(2,4-dimethylphenyl)-2,2,2-trifluoroacetohydrazide (M2)

A mixture of 3,4-diethoxybenzaldehyde (300 mg, 1.54 mmol) and (2,4-dimethylphenyl) hydrazine hydrochloride (266 mg, 1.54 mmol) in EtOH (5 mL) was stirred at room temperature for 2 h, precipitated solid was filtered off, washed with ethanol and dried under vacuum to afford hydrazone hydrochloride **2** (480 mg) in 89% yield as a white solid. The hydrazone (479 mg, 1.38 mmol) was dissolved in CH_2Cl_2 (10 mL), Et_3N (0.76 mL, 5.51 mmol) followed by $(CF_3CO)_2O$ (0.38 mL, 2.75 mmol), was added at 0 °C and the mixture was stirred at room temperature for 3 h. Reaction mixture was diluted with aq sat $NaHCO_3$ solution (20 mL), extracted with CH_2Cl_2 (2 × 30 mL), dried (Na_2SO_4) and evaporated, resulting solid was recrystallized from ethanol to give (*E*)-*N*′-(3,4-diethoxybenzylidene)-*N*-(2,4-dimethylphenyl)-2,2,2-trifluoroacetohydrazide **3** (502 mg, 80%) as a white crystals: mp 110–112 °C; ^{1}H NMR ($CDCl_3$, 500 MHz) δ ppm 1.57–1.45 (m, 6H), 2.09 (s, 3H), 2.41 (s, 3H), 4.16–4.09 (m, 4H), 6.81 (d, J = 8.5 Hz, 1H), 6.97 (dd, J = 8.5, 2.0 Hz, 1H), 7.04 (d, J = 8.0 Hz, 1H), 7.19 (m, 2H), 7.24 (s, 1H), 7.35 (s, 1H); MS (ESI): m/z calcd for $C_{21}H_{23}F_3N_2O_3$ ([M+H]$^+$) 409.1733; found 409.1781 ([M+H]$^+$).

Hydrazide **3** (439 mg, 1.07 mmol) and iodocyclohexane (0.55 mL, 4.30 mmol) in DMF (3 mL) was refluxed for 12 h. Reaction mixture was cooled and diluted with water, (10 mL), extracted with EtOAc (2 × 20 mL), washed with brine (20 mL), dried (Na_2SO_4) and evaporated, resulting solid was recrystallized from ethanol to give **M2** (200 mg, 60%) as brown crystals: mp 181–183 °C; LCMS purity 97%; ^{1}H NMR ($CDCl_3$, 500 MHz) δ ppm 2.07 (s, 3H), 2.40 (s, 3H), 5.50 (br s, OH), 5.68 (br s, OH), 6.83 (d, J = 8.0 Hz, 1H), 6.93 (dd, J = 8.0, 2.0 Hz, 1H), 7.03 (d, J = 8.0 Hz, 1H), 7.15 (s, 1H), 7.19 (d, J = 8.5 Hz, 1H), 7.23 (s, 1H), 7.30 (s, 1H); ^{13}C NMR ($CDCl_3$, 125 MHz) δ ppm 16.99, 21.29, 113.11, 115.18, 115.85, 117.52, 122.94, 127.20, 128.54, 128.70, 129.98, 132.55, 136.21, 140.88, 144.44, 144.56, 147.26; MS (ESI): m/z calcd for $C_{17}H_{15}F_3N_2O_3$ ([M+H]$^+$) 353.1107; found 353.1176 ([M+H]$^+$).

4.12. Synthesis of methyl 4-hydrazinyl-3-methylbenzoate hydrochloride (4)

To a stirred and cooled (0 °C) slurry of commercially available methyl 4-amino-3-methylbenzoate (2 g, 12.12 mmol) in 6 N HCl (12 mL) was added $NaNO_2$ (0.92 g, 13.33 mmol) in water (2 mL) drop wise maintaining a temperature of <15 °C during the addition. The mixture was stirred an additional 1.5 h affording a light yellow, homogeneous solution. To the mixture was carefully added 4.58 g (24.24 mmol) of anhydrous $SnCl_2$. The temperature during the addition was kept <10 °C. The mixture was stirred at 0 °C for 1 h. The precipitated solid was collected by filtration, dried under vacuum to afford methyl 4-hydrazinyl-3-methylbenzoate hydrochloride **4** (1.75 g 81%) as a brown solid: mp 224–226 °C; ^{1}H NMR ($CDCl_3$, 500 MHz) δ ppm 2.22 (s, 3H), 3.80 (s, 3H), 6.99 (d, J = 8.5 Hz, 1H), 7.70 (s, 1H), 7.77 (d, J = 8.5 Hz, 1H); MS (ESI): m/z calcd for $C_9H_{12}N_2O_2$ ([M+H]$^+$) 181.0932; found 181.0911 ([M+H]$^+$).

4.13. Synthesis of (*E*)-methyl 4-(2-(3-methoxybenzylidene)-1-(2,2,2-trifluoroacetyl) hydrazinyl)-3-methylbenzoate (6)

Hydrazine **4** (1 g, 4.63 mmol) and 3-methoxybenzaldehyde (629 mg, 4.63 mmol) in EtOH (15 mL) was stirred at room temperature for 5 h, precipitated solid was filtered off, washed with ethanol and dried under vacuum to afford hydrazone hydrochloride **5** (1.32 g 95%) as a white solid. This unstable hydrazone **5** (793 mg, 2.37 mmol) was dissolved in CH_2Cl_2 (20 mL), then Et_3N (1.32 mL, 9.49 mmol) followed by $(CF_3CO)_2O$ (0.66 mL, 4.75 mmol), was added at 0 °C and the mixture was stirred at room temperature for 12 h. Reaction mixture was diluted with aq sat $NaHCO_3$ solution (50 mL), extracted with CH_2Cl_2 (2 × 50 mL), dried (Na_2SO_4) and evaporated. Flash chromatography of the residue over silica gel using 5−20% EtOAc/hexane gave (*E*)-methyl 4-(2-(3-methoxybenzylidene)-1-(2,2,2-trifluoroacetyl) hydrazinyl)-3-methylbenzoate **6** (560 mg, 60%) as a thick viscous colorless syrup: ^{1}H NMR ($CDCl_3$, 500 MHz) δ ppm 2.20 (s, 3H), 3.84 (s, 3H), 3.98 (s, 3H), 6.98 (dd, J = 8.5, 2.0 Hz, 1H), 7.12 (d, J = 7.5 Hz, 1H), 7.18 (s, 1H), 7.28 (m, 3H), 8.09 (d, J = 8.0 Hz, 1H), 8.15 (s, 1H); MS (ESI): m/z calcd for $C_{19}H_{17}F_3N_2O_4$ ([M+H]$^+$) 395.1213; found 395.1230 ([M+H]$^+$).

4.14. Synthesis of (*E*)-2,2,2-trifluoro-*N*-(4-(hydroxymethyl)-2-methylphenyl)-*N*′-(3-methoxybenzylidene)acetohydrazide (M3)

To a stirred and cooled (−78 °C) solution of **6** (235 mg, 0.59 mmol) in PhMe (5 mL) was added drop wise DIBALH (1.0 M in CH_2Cl_2, 1.19 mL, 1.19 mmol). The resulting solution was stirred at this temperature for 1 h and then transferred to an ice bath for 1 h. $Na_2SO_4{\cdot}10H_2O$ (4 g) was then added, the cold bath was removed and stirring was continued for 4 h. The resulting slurry was filtered through a pad of Celite (2 × 3 cm), which was rinsed with EtOAc (3 × 10 mL). Evaporation of the solvent and flash chromatography of the residue over silica gel using EtOAc/hexane 20–50% gave **M3** (150 mg, 68%) as a dark yellow gummy syrup: ^{1}H NMR ($CDCl_3$, 500 MHz) δ ppm 2.14 (s, 3H), 3.83 (s, 3H), 4.78 (s, 2H), 6.96 (dd, J = 8.0, 2.0 Hz, 1H), 7.12 (d, J = 7.5 Hz, 1H), 7.17 (d, J = 8.0 Hz, 1H), 7.27 (m, 3H), 7.41 (d, J = 8.0 Hz, 1H), 7.46 (s, 1H); ^{13}C NMR ($CDCl_3$, 125 MHz) δ ppm 17.14, 55.26, 64.56, 111.67, 117.30, 121.00, 126.34, 129.00, 129.83, 130.17, 131.47, 134.55, 136.90, 143.56, 144.03, 159.94; MS (ESI): m/z calcd for $C_{18}H_{17}F_3N_2O_3$ ([M+H]$^+$) 367.1263; found 367.1286 ([M+H]$^+$).

Acknowledgements

We thank Professor Edward Roberts at The Scripps Research Institute for his advice and LCMS analysis. We also thank Wolfgang Fischer and William Low at Salk Institute for Mass spectral analysis. This work was supported by the Fritz B. Burns Foundation.

References and notes

1. Chen, Q.; Prior, M.; Dargusch, R.; Roberts, A.; Riek, R.; Eichmann, C.; Chiruta, C.; Akaishi, T.; Abe, K.; Maher, P.; Schubert, D. *PLoS One* **2011**, *6*, e27865.
2. Kucukguzel, S. G.; Kucukguzel, I.; Ulgen, M. *Farmaco* **2000**, *55*, 624.
3. Neumann, H. G. *Crit. Rev. Toxicol.* **2007**, *37*, 211.
4. Benigni, R.; Passerini, L. *Mutat Res.* **2002**, *511*, 191.
5. Malca-Mor, L.; Stark, A. A. *Appl. Environ. Microbiol.* **1982**, *44*, 801.
6. Rollas, S.; Kucukguzel, S. G. *Molecules* **1910**, *2007*, 12.
7. Behl, C.; Davis, J. B.; Lesley, R.; Schubert, D. *Cell* **1994**, *77*, 817.
8. Maezawa, I.; Hong, H. S.; Wu, H. C.; Battina, S. K.; Rana, S.; Iwamoto, T.; Radke, G. A.; Pettersson, E.; Martin, G. M.; Hua, D. H.; Jin, L. W. *J. Neurochem.* **2006**, *98*, 57.
9. Liu, Y.; Dargusch, R.; Maher, P.; Schubert, D. *J. Neurochem.* **2008**, *105*, 1336.
10. Ulgen, M.; Ozer, U.; Kucukguzel, I.; Gorrod, J. W. *Drug Metab. Drug Interact.* **1997**, *14*, 83.
11. Ulgen, M.; Durgun, B. B.; Rollas, S.; Gorrod, J. W. *Drug Metab. Drug Interact.* **1997**, *13*, 285.
12. Tapia-Arancibia, L.; Aliaga, E.; Silhol, M.; Arancibia, S. *Brain Res. Rev.* **2008**, *59*, 201.
13. Abe, K.; Takayanagi, M.; Saito, H. *Jpn. J. Pharmacol.* **1990**, *53*, 221.
14. McPhie, D. L.; Lee, R. K.; Eckman, C. B.; Olstein, D. H.; Durham, S. P.; Yager, D.; Younkin, S. G.; Wurtman, R. J.; Neve, R. L. *J. Biol. Chem.* **1997**, *272*, 24743.
15. LaFerla, F. M.; Green, K. N.; Oddo, S. *Nat. Rev. Neurosci.* **2007**, *8*, 499.
16. Sopher, B. L.; Fukuchi, K.; Smith, A. C.; Leppig, K. A.; Furlong, C. E.; Martin, G. M. *Brain Res. Mol. Brain Res.* **1994**, *26*, 207.
17. Davis, J. B.; Maher, P. *Brain Res.* **1994**, *652*, 169.
18. Tan, S.; Schubert, D.; Maher, P. *Curr. Top. Med. Chem.* **2001**, *1*, 497.